Electroosmotic Flow Rectification in Membranes with Asymmetrically Shaped Pores – Effects of Current and Pore Density

ARTICLE *in* THE JOURNAL OF PHYSICAL CHEMISTRY C · JUNE 2015

Impact Factor: 4.77 · DOI: 10.1021/acs.jpcc.5b03510

5 AUTHORS, INCLUDING:

James Wu

University of Florida

5 PUBLICATIONS **132** CITATIONS

THE JOURNAL OF PHYSICAL CHEMISTRY C

Article

pubs.acs.org/JPCC

Electroosmotic Flow Rectification in Membranes with Asymmetrically Shaped Pores: Effects of Current and Pore Density

Gregory W. Bishop, Marcos M. Lopez, Jr., Pradeep Ramiah Rajasekaran, Xiaojian Wu, and Charles R. Martin*

Department of Chemistry, University of Florida, Gainesville, Florida 32611-7200, United States

Supporting Information

ABSTRACT: We have recently demonstrated a new electrokinetic phenomenon—electroosmotic flow rectification in membranes with asymmetrically shaped pores. Flow rectification means that at constant driving force the flow rate in one direction through the membrane is faster than the flow rate in the opposite direction. EOF rectification could be of practical use in microfluidic devices incorporating porous membranes, but additional research is required. We explore here the effects of two key experimental variables—current density used to drive flow through the membrane and membrane pore density—on EOF rectification. We have found that the extent of EOF rectification, as quantified by the rectification ratio, increases with increasing current density. In contrast, the rectification ratio decreases with increasing membrane pore density. We propose explanations for these results based on simple EOF and membrane-transport theories.

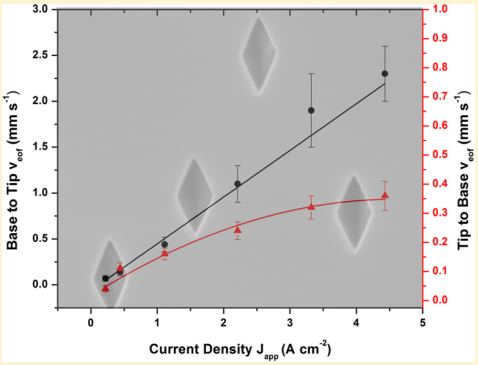

INTRODUCTION

We and others have been investigating the electrochemical and transport properties of membranes containing asymmetrically shaped pores.[1−4] Each pore in such membranes has a larger diameter opening, the base, at one face of the membrane, and a smaller diameter opening, the tip, at the opposite face. Conically shaped pores in polymeric membranes[2] and pyramidally shaped pores in mica membranes[5] are examples. We have shown that because at appropriate pH values the pore walls in the mica membranes have fixed negative charge, electroosmotic flow can be driven through the membrane.[5] This can be accomplished, for example, by passing a current through the membrane. Because the surface charge is negative, migrating double-layer cations drive electroosmotic flow (EOF), and flow is in the direction toward the cathode. We have used such experiments to demonstrate a new electrokinetic phenomenon in the pyramidal-pore membranes: electroosmotic flow rectification.[5] Flow rectification means that at constant current used to drive flow the flow rate in one direction through the membrane (base to tip) is higher than the flow rate in the opposite direction.

This EOF rectification phenomenon is of fundamental interest because it occurs only when the radius of the tip is so small that the ionic current flowing through the tip is dominated by the double layer cations. From an electrochemical point of view, this means the cation transference number in the tip must approach unity. With 10 mM electrolyte and the mica membranes used here, and in our previous studies,[5] tip diameters less than about 70 nm are required. As such, EOF rectification is a nanoscale ionics phenomenon.

EOF rectification could be of practical use in microfluidic devices incorporating porous membranes;[6] however, additional research is required. For example, while it is well-known that the velocity of EOF is proportional to current,[7] only one current was used in our prior studies.[5] In addition, membrane pore density plays a role in EOF rectification, but only one pore density was used in our prior studies.[5] We explore, for the first time, the effects of current and pore density on EOF rectification in this paper.

EXPERIMENTAL SECTION

Materials. Muscovite mica membranes (10 μm thick and 3 cm in diameter) were obtained from Spruce Pine Co. (Spruce Pine, NC). Using the linear accelerator (UNILAC) at GSI (Darmstadt, Germany), these membranes were irradiated with heavy ions to create damage tracks. Hydrofluoric acid, used to etch the damage tracks into pores, was obtained from Acros Organics (Morris Plains, NJ). For chemical vapor deposition of carbon, an ethylene/helium mixture (30% ethylene) was obtained from Praxair (Danbury, CT). Phenol was obtained from Sigma-Aldrich (St. Louis, MO). All solutions were prepared using water that was purified by passing house-distilled water through a Barnstead (Dubuque, IA) E-pure water purification system.

Etching Pyramidal Pores. A chemical etching method[5] was used to etch the damage tracks in the mica membranes into pyramidally shaped pores. This method is analogous to those used to prepare conically shaped pores in track-etch polymer membranes.[8−10] Briefly, the mica membrane was placed between

Received: April 11, 2015
Revised: June 2, 2015
Published: June 2, 2015

DOI: 10.1021/acs.jpcc.5b03510
J. Phys. Chem. C 2015, 119, 16633−16638

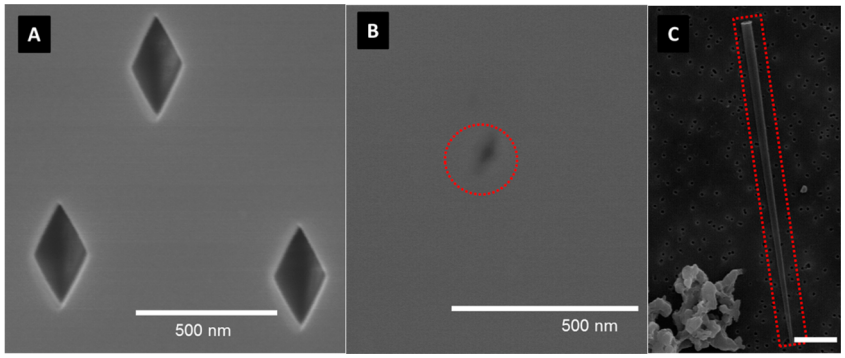

Figure 1. SEM images: (A) base openings in a track-etched pyramidal pore mica membrane; (B) tip opening in such a membrane; (C) carbon replica of a pyramidal pore (scale bar is 3 μm). Red dashed curves highlight the important parts of the images.

the two halves of an etching cell.[5,8] One side of the membrane was exposed to a 20% (v/v) HF solution while the other side was in contact with 10 M NaOH. The area of mica membrane exposed to each solution was 0.79 cm^2.[10]

Platinum wire electrodes were placed in each solution, and a Keithley 6487 picoammeter/voltage source (Cleveland, OH) was used to apply a transmembrane potential of 10 V (with the anode in the HF solution) and measure the resulting current. HF preferentially etches mica along the damage track to create a pore that ultimately breaks through to the NaOH solution on the opposite side. At room temperature (21 °C), NaOH does not etch mica at an appreciable rate, and it neutralizes the HF transported through the nascent pore from the etch solution. As a result, each pore has a small opening (tip) at one face and a large opening (base) at the opposite face. Because mica pores have a rhomboidal cross section,[11,12] these asymmetric pores are pyramidally shaped (Figure 1).[5]

Membrane Characterization. A Hitachi S-4000 field-emission scanning electron microscope (Tokyo, Japan) was used to image the rhomboidal base (Figure 1A) and tip openings (Figure 1B) and to determine the membrane pore density. Etched membranes were fractured into small pieces and adhered to scanning electron microscope (SEM) specimen mounts using double-sided carbon tape (Ted Pella, Redding, CA). Prior to SEM imaging, all samples were sputtered with Au/Pd using a Denton Vacuum Desk II (Moorestown, NJ) cold sputter instrument. The size of the long axis of the base opening was determined from images like those in Figure 1A. The size of the tip opening was determined electrochemically (*vide infra*).

Pore shape was investigated by using the template synthesis method[13] to prepare replicas of the pores. This entailed chemical-vapor deposition (CVD) of carbon along the pore walls to make rhomboidal carbon replicas that mirror the pore shape.[14] The membrane was then dissolved in 50% HF to liberate the pyramidal replicas.[5,14] The resulting mixture was filtered onto a polycarbonate membrane with 80 nm pores and was imaged from this surface (Figure 1C).

Pore density was measured by etching tracked mica with 50% HF on both sides of the membrane to obtain pores with a rhomboidal cross section, but with the same dimensions down the entire length of the pore, i.e., symmetrical pores. Etch times of 15−60 min were used to obtain large pore openings (base long-axis >300 nm). These large openings allow for low magnification images (5000× or less) that show many openings in each image (see Supporting Information). The pores in five or more such images were counted (>35 pores per image), and the average pore density was calculated.

Measurement of Pore Tip Size. The small tip openings of the pores were difficult to image (Figure 1B). Thus, the tip size was obtained by measuring the conductance of an electrolyte solution within the pores.[15] This conductance-based method is commonly used to determine the tip size of conical pores in polymeric membranes,[8,10,16] and analogous methods have been applied to mica membranes that contain symmetrical pores.[11,17,18] Briefly, a solution that was 1 M in KCl and 10 mM in phosphate buffer (pH 7.4) was placed on both sides of the mica membrane. An Ag/AgCl reference electrode was placed into each solution, and current−voltage ($I-V$) curves (associated with ion transport through the pores) were obtained (see Supporting Information file). $I-V$ curves at high electrolyte concentrations are linear (no ion-current rectification), and the slope is the membrane ionic conductance, G (in siemens, S) of the pore,[15] which is given by

$$G = (\sigma_{KCl}\pi d_b d_t)/L \quad (1)$$

where σ_{KCl} is the experimentally measured conductivity of the KCl-based electrolyte used (S cm^{-1}), L is the length of the pore (membrane thickness), d_b is the experimentally measured diameter of the base opening, and d_t is the diameter of the tip opening. Since the membrane is a collection of pyramidal conducting elements (the pores), and the base size and pore density are known from SEM measurements, the tip size can be calculated.

Ion-Current Rectification. $I-V$ curves were obtained in 10 mM phosphate buffer solutions (pH 7.4). The potential was stepped in 250 mV increments every 2 s from −10 to +10 V with respect to the electrode in the tip solution. As can be seen by the asymmetric $I-V$ curves in Figure 3, the pyramidal-pore mica membranes rectify ion current.

EOF Measurements. The membrane was mounted in the U-tube cell, and the feed half-cell was filled with 10 mM pH 7.4 phosphate buffer that was also 10 mM in the chromophore phenol. The permeate half-cell was filled with buffer. EOF was driven from feed to permeate by passing a constant current through the membrane. The electroosmotic velocity was obtained by spectrophotometrically measuring the flux of phenol across the membrane.[5] A flow through UV cell was used such that the flux across the membrane was continuously measured. Typical data are shown in Figure 2. As discussed previously, when transport is assisted by EOF, the total flux, N_i, has both diffusive and electroosmotic contributions.[5] The diffusive flux, N_{diff}, was obtained independently by doing an analogous experiment in the absence of current. Both half-cell solutions were stirred during the transport measurements.

DOI: 10.1021/acs.jpcc.5b03510
J. Phys. Chem. C 2015, 119, 16633−16638

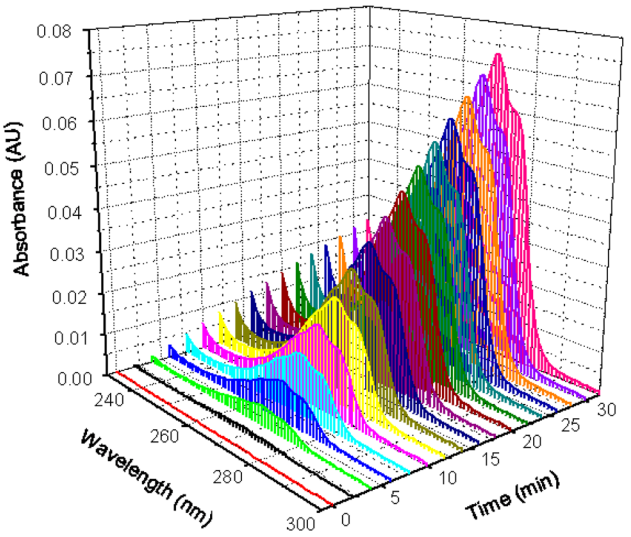

Figure 2. Continuous monitoring of phenol transport through a mica membrane containing ~10^6 pyramidal pores cm^{-2} with 100 μA applied current. Direction of phenol transport is from side of the membrane with the larger pore openings (base) to the side of the membrane with the smaller pore openings (tip).

N_i and N_{diff} were then used to calculate the enhancement factor, E[5,19]

$$E = N_i/N_{diff} \quad (2)$$

which was used to calculate the Peclet number, Pe[5]

$$E = Pe/(1 - (\exp(-Pe))) \quad (3)$$

Pe is related to electroosmotic velocity, v_{eof}, via

$$v_{eof} = PeD/l \quad (4)$$

where l is the membrane thickness and D is the diffusion coefficient for phenol.[5]

A Solartron SI1287 electrochemical interface (Hampshire, England) was used to pass the current through the membrane using Pt wires placed in the feed and permeate solutions. Since the pore walls of the mica membrane carry negative surface charge under these experimental conditions,[20] the direction of EOF was from anode to cathode.[5] Thus, the experiment was configured such that the working electrode (anode) was in the feed solution and the reference/counter electrode (cathode) was in the permeate solution.

RESULTS AND DISCUSSION

Membranes Studied. The length of the long axis of the rhomboidal pore opening (Figure 1A) was used to characterize the pore size.[5] From the SEM images, the long axis of the base opening was found to be 330 ± 12 nm. It is difficult to image the smaller tip opening by SEM (Figure 1B); however, such images yielded a value for the long axis of the tip of ~40 nm. This is in good agreement with the more accurate electrochemically determined value of 39 ± 3 nm. The entire pore can be visualized through images of the carbon replicas prepared in these pores (Figure 1C). Membranes with two different pore densities were used for these studies; SEM images yielded pore-density values of 1.0(±0.1) × 10^6 cm^{-2} and 9(±1) × 10^6 cm^{-2}, which correspond well to the track densities of 10^6 and 10^7 cm^{-2} reported by the supplier. For simplicity, the membranes are identified by their nominal pore densities, 10^6 and 10^7 pores cm^{-2}.

Theory of EOF and Ion-Current Rectification. Membranes with asymmetrically shaped pores, such as the pyramidal pores studied here, offer two directions for EOF-assisted transport through the membrane—transport from the base side to the tip side or transport from the tip side to the base side. In our prior studies we showed that at the same current used to drive flow through the membrane the rate of EOF transport from base-to-tip was higher than the rate from tip-to-base[5]—EOF rectification.

We discussed the theory of membrane EOF rectification previously.[5] Briefly, EOF rectification occurs for the same reason that ion current is rectified in these membranes (Figure 3). Both

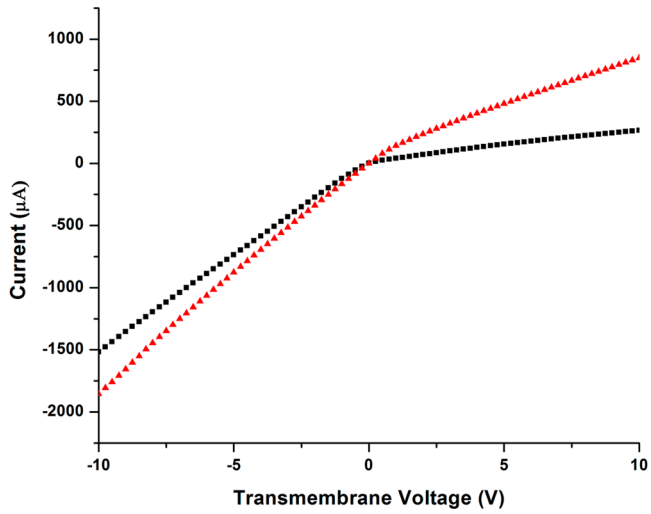

Figure 3. Current—voltage curves for pyramidal-pore mica membranes with pore densities of 10^6 cm^{-2} (black squares) and 10^7 cm^{-2} (red triangles).

phenomena require that the pore wall is charged, and there is negative surface charge on mica.[20] As a result of this surface charge, when immersed into an electrolyte solution, an electrical double layer forms at the pore wall.[21] This is the portion of solution immediately adjacent to the wall that contains the excess cations required to balance the negative surface charge. EOF occurs through the membrane in the direction toward the cathode because of these mobile double-layer cations.

According to a prevailing theory, if the radius of the tip is sufficiently small such that the cation transference number in the tip approaches unity, passing an ionic current through the pore alters the electrolyte concentration within the tip region of the pore.[22] Specifically, when the cathode is in the solution facing the tip (corresponding to base-to-tip EOF), electrolyte is depleted from the tip region. This current-induced depletion causes the ionic resistivity, ρ, of the pore to increase. In contrast, when the cathode is in the solution facing the base (tip-to-base EOF), electrolyte accumulates in the tip causing ρ to decrease.

This increase or decrease in tip-solution ionic resistivity, depending on the direction of the current passing through the membrane, is responsible for both ion-current and EOF rectification. The higher ρ value obtained when the polarity is such that the cathode is in the solution facing the tip produces the low current state observed at positive applied transmembrane voltages (Figure 3). Likewise, the lower ρ value obtained when

DOI: 10.1021/acs.jpcc.5b03510
J. Phys. Chem. C 2015, 119, 16633−16638

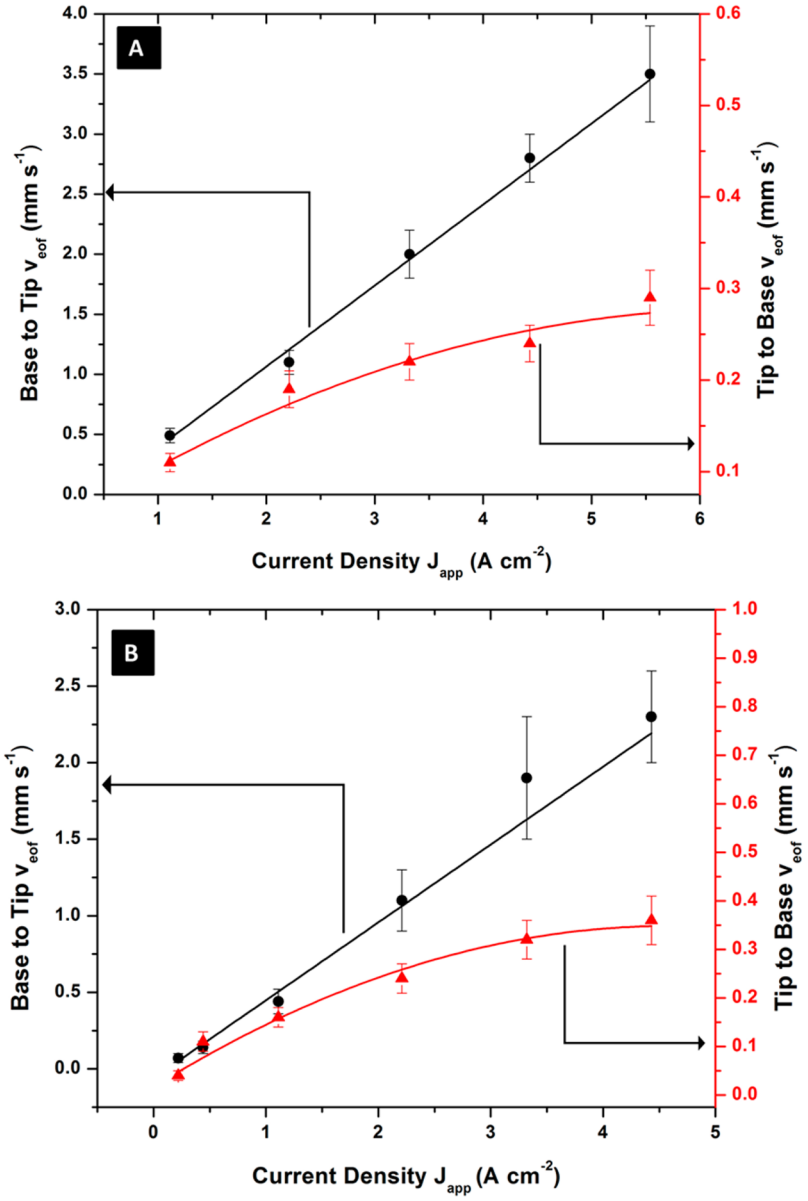

Figure 4. Plots of EOF velocity (v_{eof}) vs current density (J_{app}) for membranes with pore densities of (A) 10^6 cm^{-2} and (B) 10^7 cm^{-2}. In each case the left *y*-axis is for faster base-to-tip EOF, and the right *y*-axis is for slower tip-to-base transport. The error bars represent the standard deviation obtained from three consecutive trails on the same membrane.

the cathode is in the solution facing the base yields the high current state observed at negative voltages.

These current-induced changes in tip-solution resistivity are responsible for EOF rectification because EOF velocity is to a first approximation (*vide infra*), proportional to ρ[19]

$$v_{eof} = -\varepsilon\zeta J_{app}\rho/\eta \quad (5)$$

where ε and η are the permittivity and viscosity of the solution, respectively, J_{app} is the current density, and ζ is the zeta potential of the charged pore wall. Equation 5 predicts that the high solution ρ associated with base-to-tip transport will produce a high v_{eof} state and the low solution ρ associated with tip-to-base transport will produce a low v_{EOF} state, and this is what we observed experimentally.[5] Both the 10^7 and 10^6 pores cm^{-2} membranes studied here showed EOF rectification. This can be demonstrated through plots of v_{eof} vs J_{app} (Figure 4), where for both membranes, and at all current densities, v_{eof} base-to-tip is higher than v_{eof} tip-to-base.

Effect of Current Density. The extent of EOF rectification at any current density can be quantified by the EOF rectification ratio (r_{eof}) defined as v_{eof} base-to-tip divided by v_{eof} tip-to-base.[5] For both membranes, r_{eof}, in general, increases with increasing current density (Table 1). The maximum value obtained for the 10^6 pores cm^{-2} membrane was $r_{eof} = 12 \pm 2$, while the maximum for the 10^7 pores cm^{-2} membrane was 6 ± 1.

In order to understand these data, it is important to refine eq 5 to account for both the resistivity of the double layer cations (ρ_{dl}) and the resistivity of the bulk electrolyte incorporated into the pore as a result of accumulation (ρ_{bk}) to the total pore resistivity (ρ). Because these two resistances are in parallel, they sum as per eq 6:

DOI: 10.1021/acs.jpcc.5b03510
J. Phys. Chem. C 2015, 119, 16633−16638

Table 1. Effect of Current Density on EOF Rectification Ratio (r_{eof}) for membranes with 10^6 and 10^7 pore cm^{-2}

current density, J_{app}[a] (A cm^{-2})	r_{eof} 10^6 pores cm^{-2} membrane	r_{eof} 10^7 pores cm^{-2} membrane
0.22		1.8 ± 0.9
0.44		1.3 ± 0.4
1.11	4.5 ± 0.8	2.8 ± 0.7
2.21	5.8 ± 0.9	4.7 ± 0.9
3.32	9 ± 1	6 ± 1
4.43	12 ± 1	6 ± 1
5.54	12 ± 1	

[a]The current density was calculated based on the geometric mean of the base and tip openings of the pore.

$$\frac{1}{\rho} = \frac{1}{\rho_{(dl)}} + \frac{1}{\rho_{(bk)}} \quad (6)$$

Replacing ρ in eq 5 results in eq 7

$$v_{eof} = -\varepsilon\zeta J_{app}\rho_{(dl)}/(1 + [\rho_{(dl)}/\rho_{(bk)}])\eta \quad (7)$$

In depletion mode (corresponding to faster base-to-tip EOF in Figure 4), $\rho_{(bk)} \gg \rho_{(dl)}$, and eq 7 becomes

$$v_{eof} = -\varepsilon\zeta J_{app}\rho_{(dl)}/\eta \quad (8)$$

Because $\rho_{(dl)}$ is independent of current density, eq 8 predicts that v_{eof} is linearly related to J_{app} in depletion mode. In agreement with this analysis, reasonable linear fits were obtained for both the 10^6 pores cm^{-2} membrane (Adj-R^2 = 0.990) and 10^7 pores cm^{-2} membrane (Adj-R^2 = 0.978) membranes (Figure 4). This analysis assumes that the zeta potential is also a constant in eq 8. This assumption is valid because we are in depletion mode and it is well-known that ζ becomes constant at low electrolyte concentrations.[23]

In accumulation mode (corresponding to slower tip-to-base EOF in Figure 4), $\rho_{(dl)} \gg \rho_{(bk)}$, and eq 7 becomes

$$v_{eof} = -\varepsilon\zeta J_{app}\rho_{(bk)}/\eta \quad (9)$$

Since the quantity of electrolyte accumulated in the tip region of the pore is proportional to the current flowing through the pore, $\rho_{(bk)}$ should decrease with increasing current density. Hence, the linear relationship between v_{eof} and J_{app} observed in depletion mode is not expected. This lack of linear dependence is exacerbated by the effect of accumulation on the zeta potential. Increasing the electrolyte concentration in the tip region will cause ζ in eq 9 to decrease; indeed, at high electrolyte concentrations, ζ approaches zero,[24] which would turn off EOF. These effects of accumulation of electrolyte on $\rho_{(bk)}$ and ζ suggest that plots of v_{eof} vs J_{app} should be nonlinear in accumulation mode, and this is what we observe experimentally (Figure 4). This can be demonstrated by the lower linear-fit correlation coefficients for both the 10^6 pores cm^{-2} membrane (Adj-R^2 = 0.937) and 10^7 pores cm^{-2} membrane (Adj-R^2 = 0.909). These poorly fitting straight lines are not shown in Figure 4 for the accumulation/tip-to-base case. Instead, the lines are for parabolic fits. Finally, because v_{eof} increases linearly with J_{app} in depletion/base-to-tip mode whereas the relationship is nonlinear for the accumulation/tip-to-base case, r_{eof} increases with increasing current density (Table 1).

Effect of Pore Density. We found in Table 1 that r_{eof} is less for the 10^7 pores cm^{-2} membrane than for the 10^6 pores cm^{-2} membrane. To understand why this is so, we compared the tip-to-base and the base-to-tip EOF velocities for these two membranes at a constant current density of 3.32 A cm^{-2}. The base-to-tip velocities were identical, 2 mm s^{-1}. In contrast, the tip-to-base v_{eof} for the 10^7 pores cm^{-2} membrane was 0.32 mm s^{-1}, larger than the value for the 10^6 pores cm^{-2} membrane, 0.22 mm s^{-1}. Because in the calculation of the rectification ratio the tip-to-base EOF velocity is in the denominator, the higher velocity for the 10^7 pores cm^{-2} membrane explains empirically why the rectification ratio is lower for this membrane.

To understand why the tip-to-base EOF velocity is lower for the 10^6 pores cm^{-2} membrane, we did a detailed analysis of the voltage drop across each membrane at the constant current density of 3.32 A cm^{-2}. The key point in this analysis is that the total resistance of the cell has contributions from the solutions on either side of the membrane and the membrane itself. In depletion mode the membrane resistance dominates, and the solution resistance can be ignored. This is not true in accumulation mode where due to the lower membrane resistance, the solution resistance dominates. We obtained an independent measure of the solution resistance by obtaining current voltage curves in the absence of the membrane.

At J_{app} = 3.32 A cm^{-2}, the currents forced through the 10^7 pores cm^{-2} and 10^6 pores cm^{-2} membranes are 750 and 75 μA, respectively. For tip to base EOF (accumulation mode), the total cell resistance for the 10^7 pores cm^{-2} membrane was 5390 Ω, of which 4860 Ω came from the solutions and 530 Ω from the membrane. From the known current and total cell resistance, Ohm's law shows that 4 V was applied across the membrane to supply the 750 μA current for the 10^7 pores cm^{-2} membrane. Of this total 4 V, the known membrane resistance value shows that 0.4 V is dropped across the membrane itself.

For tip to base EOF (accumulation mode) at the 10^6 pores cm^{-2} membrane, the total cell resistance was 6500 Ω, of which 4860 Ω came from the solutions and 1640 Ω from the membrane itself. Ohm's law in this case indicates that 0.5 V was applied across the membrane to supply the 75 μA current for the 10^6 pores cm^{-2} membrane. Of this 0.5 V total, 0.13 V was dropped across the membrane.

We learn from this analysis that even though the current density was the same for both membranes, the voltage drops across the membranes are not the same. The voltage drop across the 10^7 pores cm^{-2} membrane is higher. This means that the electric field gradient across the 10^7 pores cm^{-2} membrane is higher. Since the velocity of EOF scales with the electric field gradient, this explains the higher v_{eof} in accumulation mode for the 10^7 pores cm^{-2} membrane (*vide supra*). And this explains why the rectification ratio is lower for this membrane (Table 1).

CONCLUSIONS

We have reported here the first investigation of applied current density and membrane pore density on electroosmotic flow rectification in asymmetrical pore membranes. We have found that when EOF is in the direction from base-to-tip electroosmotic velocity is linearly related to current density (eq 8). In contrast, when EOF is in the direction from tip-to-base electroosmotic velocity shows a nonlinear relationship with current density, falling off at the highest current densities (Figure 4). This causes the rectification ratio, r_{eof}, to increase with increasing current density (Table 1). We have also found that EOF rectification ratios for a membrane with 10^6 pores cm^{-2} are higher than r_{eof} values for a membrane with 10^7 pores cm^{-2}. We have shown that this is because, at the same current density, a higher voltage is dropped across the 10^7 pores cm^{-2} membrane.

DOI: 10.1021/acs.jpcc.5b03510
J. Phys. Chem. C 2015, 119, 16633−16638

This causes the tip-to-base EOF velocity for the 10^7 pores cm^{-2} membrane to be higher, and this accounts for the lower rectification ratio for this membrane.

The practical consequences of this work stem from the possibility of using such asymmetric-pore membranes in microfluidic devices[6] and as pumps for such devices. Our results suggest that passing an alternating current (ac) through the membrane will yield a net flow in the direction base opening to tip opening. This is because in one-half-cycle the polarity would be such that high velocity flow occurs base-to-tip, whereas in the opposite half cycle a lower flow rate would be directed tip-to-base. While current microfluidic devices use a constant applied voltage to achieve a direct current (dc) through the device,[6] there is much interest in using ac instead.[25,26] This is because the dc mode requires that thermodynamically uphill redox reactions be driven at each electrode in the device. This consumes power and leads to unwanted pH changes in the solutions contacting the electrodes.[25,26] In ac mode no redox reactions occur at the electrodes, and this should obviate both of these problems. Because we observed a higher rectification ratio for the lower pore density membrane, a higher net flow rate should be obtained for such membranes.

■ ASSOCIATED CONTENT

Supporting Information

Figure S1: two typical electron micrographs used to determine the pore density of the 10^7 pores cm^{-2} membranes; Figure S2: typical current−voltage (I−V) curve used to determine the diameter of the tip opening for a 10^6 pores cm^{-2} membrane. The Supporting Information is available free of charge on the ACS Publications website at DOI: 10.1021/acs.jpcc.5b03510.

■ AUTHOR INFORMATION

Corresponding Author

*Phone 352-392-8205; Fax 352-392-8206; e-mail crmartin@chem.ufl.edu (C.R.M.).

Present Addresses

G.W.B.: Department of Chemistry, University of Connecticut, Storrs, CT 06269-3060.

M.M.L.: Columbia University College of Physicians and Surgeons, 630 West 168th Street, New York, NY 10032.

Funding

The work was supported by the Nanostructures for Electrical Energy Storage (NEES), an Energy Frontier Research Center funded by the US Department of Energy, Office of Science, Office of Basic Energy Sciences, under Award DESC0001160.

Notes

The authors declare no competing financial interest.

■ REFERENCES

(1) Siwy, Z.; Troffin, L.; Kohli, P.; Baker, L. A.; Trautmann, C.; Martin, C. R. Protein Biosensors Based on Biofunctionalized Conical Gold Nanotubes. *J. Am. Chem. Soc.* **2005**, *127*, 5000−5001.

(2) Siwy, Z.; Heins, E.; Harrell, C. C.; Kohli, P.; Martin, C. R. Conical Nanotube Ion-Current Rectifiers − The Role of Surface Charge. *J. Am. Chem. Soc.* **2004**, *126*, 10850−10851.

(3) Mara, A.; Siwy, Z.; Trautmann, C.; Wan, J.; Kamme, F. An Asymmetric Polymer Nanopore for Single Molecule Detection. *Nano Lett.* **2004**, *4*, 497−501.

(4) Siwy, Z. Ion-Current Rectification in Nanopores and Nanotubes with Broken Symmetry. *Adv. Funct. Mater.* **2006**, *16*, 735−746.

(5) Jin, P.; Mukaibo, H.; Horne, L. P.; Bishop, G. W.; Martin, C. R. Electroosmotic Flow Rectification in Pyramidal-Pore Mica Membranes. *J. Am. Chem. Soc.* **2010**, *132*, 2118−2119.

(6) Kuo, T.-C.; Cannon, D. M., Jr.; Chen, Y.; Tulock, J. J.; Shannon, M. A.; Sweedler, J. V.; Bohn, P. W. Gateable Nanofluidic Interconnects for Multilayered Microfluidic Separation Systems. *Anal. Chem.* **2003**, *75*, 1861−1867.

(7) Brydges, T. G.; Lorimer, J. W. The Dependence of Electro-osmotic Flow on Current Density and Time. *J. Membr. Sci.* **1983**, *13*, 291−305.

(8) Apel, P. Y.; Korchev, Y. E.; Siwy, Z.; Spohr, R.; Yoshida, M. Diode-like Single-ion Track Membrane Prepared by Electro-Stopping. *Nucl. Instrum. Methods Phys. Res., Sect. B* **2001**, *184*, 337−346.

(9) Siwy, Z.; Dobrev, D.; Neumann, R.; Trautmann, C.; Voss, K. Electro-Responsive Asymmetric Nanopores in Polyimide with Stable Ion Current Signal. *Appl. Phys. A: Mater. Sci. Process.* **2003**, *76*, 781−785.

(10) Wharton, J. E.; Jin, P.; Sexton, L. T.; Horne, L. P.; Sherrill, S. A.; Mino, W. K.; Martin, C. R. A Method for Reproducibly Preparing Synthetic Nanopores for Resistive-Pulse Biosensors. *Small* **2007**, *3*, 1424−1430.

(11) Bean, C. P.; Doyle, M. V.; Entine, G. Etching of Submicron Pores in Irradiated Mica. *J. Appl. Phys.* **1970**, *41*, 1454−1459.

(12) Khan, H. A.; Khan, N. A.; Spohr, R. Scanning Electron Microscope Analysis of Etch Pits Obtained in a Muscovite Mica Track Detector by Etching in Hydro-Fluoric Acid and Aqueous Solutions of NaOH and KOH. *Nucl. Instrum. Methods* **1981**, *189*, 577−581.

(13) Martin, C. R. Nanomaterials: A Membrane-Based Synthetic Approach. *Science* **1994**, *266*, 1961−1966.

(14) Xu, F.; Wharton, J. E.; Martin, C. R. Template Synthesis of Carbon Nanotubes with Diamond-Shaped Cross Sections. *Small* **2007**, *3*, 1718−1722.

(15) Apel, P. Y.; Ramirez, P.; Blonskaya, I. V.; Orelovitch, O. L.; Sartowska, B. A. Accurate Characterization of Single Track-etched, Conical Nanopores. *Phys. Chem. Chem. Phys.* **2014**, *16* (29), 15214−15223.

(16) Sexton, L. T.; Horne, L. P.; Sherrill, S. A.; Bishop, G. W.; Baker, L. A.; Martin, C. R. Resistive-Pulse Studies of Proteins and Protein/Antibody Complexes Using a Conical Nanotube Sensor. *J. Am. Chem. Soc.* **2007**, *129*, 13144−13152.

(17) Anderson, J. L.; Quinn, J. A. Ionic mobility in Microcapillaries. A Test for Anomalous Water Structures. *J. Chem. Soc., Faraday Trans. 1* **1972**, *68*, 744−748.

(18) Quinn, J. A.; Anderson, J. L.; Ho, W. S.; Petzny, W. J. Model Pores of Molecular Dimension. *Biophys. J.* **1972**, *12*, 990−1007.

(19) Miller, S. A.; Young, V. Y.; Martin, C. R. Electroosmotic Flow in Template-Prepared Carbon Nanotube Membranes. *J. Am. Chem. Soc.* **2001**, *123*, 12335−12342.

(20) Fröhlich, H. P.; Woermann, D. Modification of Electrochemical Properties of Pore Wall of Track-Etched Mica Membranes. *Colloid Polym. Sci.* **1986**, *264*, 159−166.

(21) Bard, A. J.; Faulkner, L. R. *Electrochemical Methods: Fundamentals and Applications*, 2nd ed.; Wiley: New York, 2001; p 12.

(22) Cervera, J.; Schiedt, B.; Ramírez, P. A Poisson/Nernst-Planck Model for Ionic Transport through Synthetic Conical Nanopores. *Europhys. Lett.* **2005**, *71*, 35−41.

(23) Galembeck. F. *Surface and Colloidal Science: Progress in Colloid and Polymer Science*; Springer-Verlag: Berlin, 2004; Vol. *128*, p 5.

(24) Goel, A. *Colloidal Chemistry*; Discovery Publishing House: New Delhi, 2006; p 58.

(25) Huang, C. C.; Bazant, M. Z.; Thorsen, T. Ultrafast High-Pressure AC Electro-osmotic Micropumps for Portable Biomedical Microfluidics. *Lab Chip* **2010**, *10*, 80−85.

(26) Brask, A.; Snakenborg, D.; Kutter, J. P.; Bruus, H. AC Electroosmotic Pump with Bubble-free Palladium Electrodes and Rectifying Polymer Membrane Valves. *Lab Chip* **2006**, *6*, 280−288.

DOI: 10.1021/acs.jpcc.5b03510
J. Phys. Chem. C 2015, 119, 16633−16638